DOI: 10.1002/ejic.200800622

1,2-Diboracyclopentanes without Strong Donor Substituents: Synthesis, Reactions, and Computational Analysis

Carsten Präsang,[a] Yüksel Sahin,[b] Matthias Hofmann,[c] Gertraud Geiseler,[a] Werner Massa,[a] and Armin Berndt*[a]

Keywords: Ab initio computations / Boron / Kinetically preferred reactions / Rearrangements

The 1,2-diduryl-1,2-diboracyclopentane **1a** was obtained in good yield from the recently described 1,2-dichloro-1,2-diboracyclopentane **1c**. Thermolysis of **1a** led to a mixture of compounds from which degradation products **5a** and **6a** as well as isomer **7a** could be isolated. Sterically less-hindered **1b** spontaneously transformed into its isomer **7b**. Attempts to prepare **4a** by deprotonation of **1a** led to ring enlarged anions **8a** and **8b**. The structures of all new compounds were definitively proven by X-ray structural analyses. Computations at the B3LYP/6-311+G** level of theory suggest that derivatives of the kinetically preferred isomer **2u** of **1u** are the key intermediates on the route to **5a** and **6a**, which are the main products of the thermolysis of **1a**. In contrast to expectation, derivatives of thermodynamically preferred isomer **3u** could neither be observed nor shown by computations to be involved in the formation of the products obtained from **1a** and **1b**.

Introduction

1,2-Diboracyclopentanes with strong donor substituents at the boron centers[1,2] do not show any tendency to form nonclassical isomers. The latter have been computed to be preferred energetically in case of unsubstituted prototype **1u** (Scheme 1): monohomoaromatic **2u** and bishomoaromatic **3u** are lower in energy than **1u** by 2.5 and 18.9 kcal mol^{-1}, respectively, at the MP2/6-31G* level of theory.[3] Recent computations revealed **3u** to be the strongest neutral homoaromatic ever discussed, 50.5 kcal mol^{-1} lower in energy than **3u***, which does not feature a three-center-two-electron BCB bond.[4] Formation of derivatives of isoelectronic species **B** and **E** by isomerization of the corresponding derivatives of **A** and **D**, respectively, have been observed.[4,5] Compounds of type **E** were also obtained by protonation of derivatives of **F**.[6]

Therefore, we expected derivatives of **3u** to be accessible from the corresponding derivatives of **1u** and **4u**. Because the latter is a bishomoaromatic stabilized by 54 kcal mol^{-1} (at the MP4/6-311+G** level)[7–9] relative to its classical isomer with the negative charge localized at a carbon center, we hoped to be able to synthesize derivatives of it by deprotonation of derivatives of **1u**. Nonclassical 1,2,4-triboracyclopentanes of type **C**, monohomoaromatic like **2u**, were recently reported to form spontaneously from their classical isomers.[10]

[a] Fachbereich Chemie der Universität Marburg,
Hans-Meerwein-Strasse, 35032 Marburg
Fax: +49-6421-2828917
E-mail: berndta@staff.uni-marburg.de
[b] Adnan Menderes University, Faculty of Science & Arts,
Chemistry Department,
09010 Aydın, Turkey
[c] Anorganisch-Chemisches Institut der Universität Heidelberg,
Im Neuenheimer Feld 270, 69120 Heidelberg
E-mail: matthias.hofmann@aci.uni-heidelberg.de

Results and Discussion

Syntheses and NMR Spectroscopic Results

Reaction of the 1,2-dichloro-1,2-diboracyclopentane **1c**[2] with duryllithium afforded **1a** in 90% yield (Scheme 2).

Upon melting of **1a** or heating solutions of **1a** at reflux in benzene, a mixture of compounds was obtained from which nonclassical diborirane **5a** could be isolated as the main product (55–60%). *trans*-1,2-Bis(trimethylsilyl)ethene, which is formed as a byproduct of **5a**, was unambiguously identified by NMR spectroscopy. Borylmethyleneborane **6a** and isomer **7a** of **1a** were obtained in 12–25 and 5% yield, respectively. The 1,2-diboracyclopentane **1b** could not be crystallized after **1c** was allowed to react with (3,5-di-*tert*-butylphenyl)lithium, but crystals of its isomer **7b** were obtained in 63% yield. Attempts to generate **4a** by deprotonation of **1a** by using bases like mesityllithium and LDA were unsuccessful, probably due to steric hindrance. Reaction of **1a** with *n*-butyllithium in diethyl ether did not lead to **4a** but to solvent separated ion pair **8a**·Li(Et$_2$O)$_n$. Solutions of contact ion pair **8b**·Li(Et$_2$O) were obtained by exchanging the solvent for *n*-pentane or [D$_6$]benzene (Scheme 3). Obviously, addition of the butyl anion to the

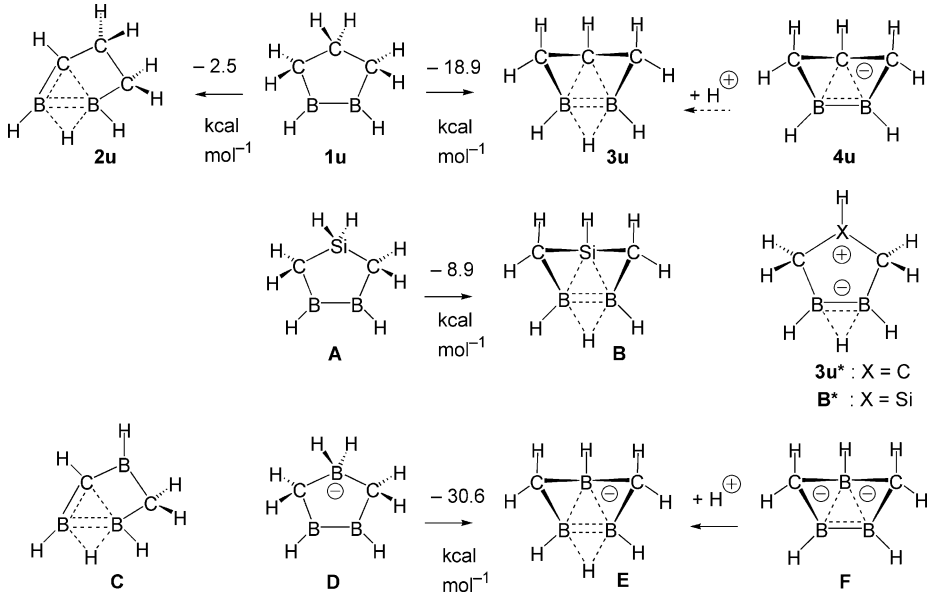

Scheme 1. Energy differences [kcal mol^{-1}, computed at the MP2(fc)/6-31G* + 0.93ZPE level of theory] between isoelectronic classical five membered rings **1u**, **A**, and **D** and their bishomoaromatic isomers **3u**, **B**, and **E**, the monohomoaromatic isomer **2u** of **3u**, as well as alternative routes to **3u** and **E**.

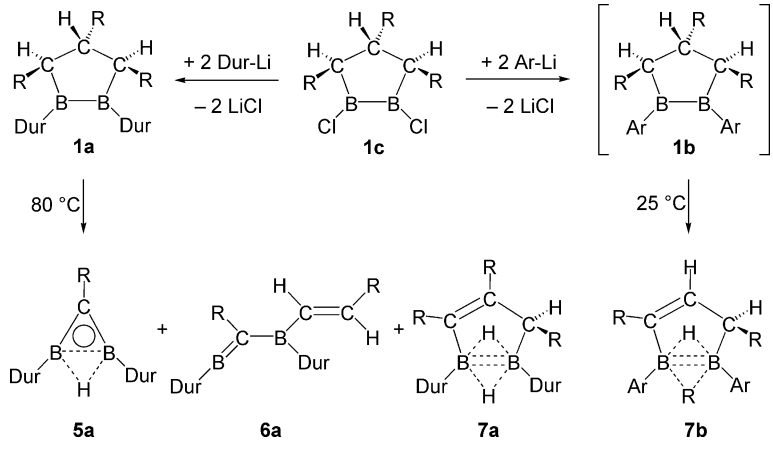

Scheme 2. Synthesis of **1a** from **1c** and products **5a**, **6a**, and **7a** obtained by thermolysis of **1a**, as well as formation of **7b** upon the attempted synthesis of **1b** (R = $SiMe_3$, Dur = 2,3,5,6-tetramethylphenyl, Ar = 3,5-di-*tert*-butylphenyl).

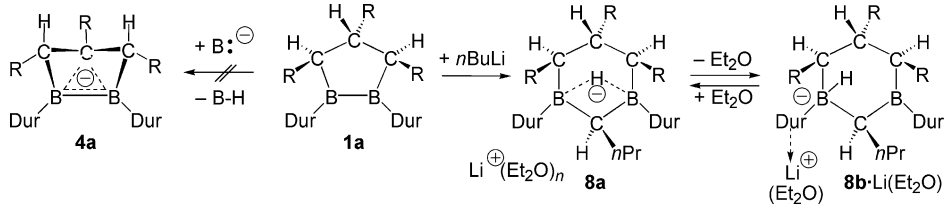

Scheme 3. Reaction of **1a** with *n*-butyllithium does not lead to deprotonation product **4a** but to addition products **8a**·Li(Et_2O)$_3$ or **8b**·Li(Et_2O) depending on the workup conditions.

B–B moiety – with subsequent rearrangement – is faster than its action as a base, in spite of the strong thermodynamic stabilization of anions of type **4**.

The constitution of most of the new compounds was definitively proven by their X-ray structural analyses described below. The NMR spectroscopic data of the new compounds given in the Experimental Section are in full agreement with expectations. Thus, the signal at $\delta(^{11}B)$ = 29 ppm for **5a** is identical to that of a known nonclassical diborirane derivative containing a dimethylphenylsilyl and a bis(trimethylsilyl)methyl substituent instead of the trimethylsilyl and one duryl substituent, respectively, in **5a**.[11] Notably, the proton of the BHB bridge of aromatic diborirane **5a** [$\delta(^1H)$ = 8.47 ppm] is considerably deshielded rela-

tive to the signals for the BHB bridges in nonaromatic **7a**,**b** [$\delta(^1H)$ = 2.53, 3.63, 2.9 ppm]. The NMR spectra of borylmethyleneborane **6a** are strongly dependent on temperature. Even at –90 °C, the number of signals to be expected for **6a** could not be observed. The averaged signal belonging to the *para*-carbon atoms of the two duryl substituents shows line broadening below –70 °C and coalescence at about –90 °C. This indicates an intramolecular exchange process that we assigned to topomerization by migration of the β-trimethylsilylvinyl substituent from the tricoordinate to the dicoordinate boron center. A similar topomerization by migration of a γ-bis(trimethylsilyl)-α-ethylallenyl substituent in the related 1,3-diduryl-2-ethylborylmethyleneborane **G** (see Scheme 5) has been described before.[12] The barrier height of the topomerization of **6a** can be estimated to be 8 kcal mol^{-1} by using the chemical shift difference of 6–7 ppm as measured for the *para*-carbon centers of similar 1,3-diduryl-2-borylmethyleneboranes.[12] The ^{11}B NMR chemical shift of **7a** (δ = 23 ppm) corresponds to δ = 21.8 ppm described for closely related 1,2-trimethylenediborane(6).[13] Only one ^{11}B NMR signal at δ = 21 ppm is observed for both boron centers of **8b**·Li(Et_2O) in *n*-pentane or [D_6]benzene. This indicates a fast exchange of the hydride between the tricoordinate and tetracoordinate sites in solution [**8a**·Li(Et_2O)$_n$ in diethyl ether: 3 ppm, both boron centers tetracoordinate].

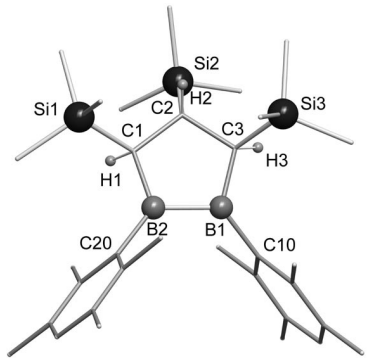

Figure 1. Structure of **1a** in the crystal; most of the hydrogen atoms have been omitted for clarity. Selected bond lengths [pm] and angles [°]: B1–B2 174.8(3), B2–C1 156.4(3), C1–C2 157.7(2), C2–C3 158.1(2), C3–B1 154.8(3), B1–C10 158.1(3), B2–C20 157.6(3), C1–Si1 189.7(2), C2–Si2 191.1(2), C3–Si3 190.1(2); B1–B2–C1 104.1(1), B1–B2–C20 129.8(2), B2–B1–C3 105.2(1), B2–B1–C10 128.7(2), B1–C3–C2 109.7(1), C3–C2–C1 108.4(1), C2–C1–B2 110.4(1), B2–C1–C2–C3 –0.1(2), C1–B2–B1–C3 14.5(2).

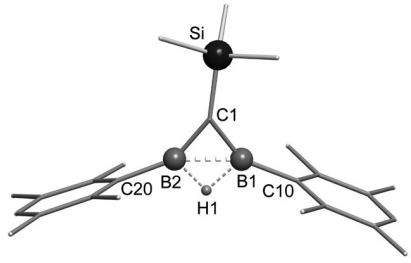

Figure 2. Structure of molecule **5a** in the crystal, most of the hydrogen atoms have been omitted for clarity. Selected bond lengths [pm] and angles [°]: B1–B2 173.3(2), B2–C1 144.4(2), C1–B1 143.9(2), B1–C10 156.5(2), C1–Si1 183.5(2), B2–C20 156.0(2), B1–C1–B2 73.9(1), B1–H1 126(2), B2–H1 127(2); B1–H1–B2 86(1), C1–B1–B2 53.2(1), C1–B2–B1 52.9(1), C1–B1–C10 149.4(2), C1–B2–C20 148.6(1), B1–C1–Si1 147.6(1), B2–C1–Si1 138.5(1).

Crystal Structures

Figures 1–7 show the structures of **1a**, **5a**, **6a**, **7a**,**b**, **8a** and **8b**·Li(Et_2O) in the crystal.

The structure of **1a** (Figure 1) resembles that of **1c**,[2] differences can be explained by increased steric hindrance and reduced hyperconjugation in **1a** relative to those in **1c**. Compound **1a** deviates strongly from C_s symmetry in the solid state mainly due to the positions of the duryl moieties. The five-membered ring shows an envelope conformation with a folding angle at the B2···C3 axis of 165.1(1)°. Therefore, C20 is above and C10 is below the ring plane in Figure 1 (see also caption).

Compound **5a** (Figure 2) is the simplest derivative of a nonclassical diborirane to be characterized by X-ray structural analysis. The distances within the ring are close to those computed for prototype **5u**.[10] The molecule deviates in the crystal from C_s symmetry mainly by an inclination of the $SiMe_3$ group toward C10, as documented in the differing B–C1–Si angles and by a rotation of the $SiMe_3$ group around the C1–Si axis by 9.3(2)° out of the ideal position.

Compound **6a** (Figure 3) is the borylmethyleneborane[14] with the lowest steric hindrance so far characterized by X-ray structural analysis. This allows for the first time to study geometrical influences of π–π and σ–π delocalization undisturbed by steric and additional electronic effects.[15] The C1–B2 bond is significantly shorter than the B2–C2 bond. This clearly indicates delocalization of the π electrons of the C1–B1 bond to the formally empty p orbital at B2, which increases the electron deficiency of the empty p orbital at B1 in the plane of the molecule.[14] As a consequence, strong hyperconjugation of this orbital with the C1–Si1 bond gives rise to a bond angle B1=C1–Si1 of only 114°, considerably smaller than the C2=C3–Si2 bond angle of 125°. A C=C–Si bond angle of 115° was recently observed for the first vinyl cation to be characterized by X-ray structural analysis and explained by strong C–Si hyperconjugation.[16] Vinyl cations are isoelectronic with methyleneboranes.[14]

The five-membered rings of the precursors are retained in **7a**,**b** (Figures 4 and 5); however, two hydrogen atoms or one hydrogen and a trimethylsilyl group, respectively, originally attached to carbon are found now as bridges between the boron centers. The B–B distances in **7a** and **7b** are comparable to those in diboranes(6).[17] The C1–C2 double bond in **7a** is significantly longer than in **7b** and more twisted (difference of torsions B2–C1–C2–C3 7.8°). This can be explained by steric hindrance between the two *Z*-configured trimethylsilyl substituents in **7a**. The B–Si distances of the BSiB bridge in **7b** are very similar to that of Calabrese's pentaborane with a silyl bridge.[18] To the best of our knowledge, molecules containing a BSiB bridge in

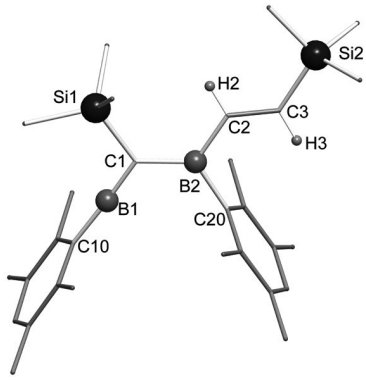

Figure 3. Structure of molecule **6a** in the crystal, most of the hydrogen atoms have been omitted for clarity. Selected bond lengths [pm] and angles [°]: C1–B1 137.9(3), C1–B2 153.3(3), B2–C2 157.0(3), C2–C3 132.7(3), B1–C10 151.2(3), C1–Si1 185.8(2), B2–C20 159.0(3), C3–Si2 187.3(2); B1–C1–B2 121.5(2), B1–C1–Si1 114.0(1), C1–B1–C10 177.4(2), C1–B2–C2 120.9(2), C1–B2–C20 121.9(2), B2–C2–C3 127.1(2), C2–C3–Si2 125.5(2), B1–C1–B2–C2 178.4(2), C1–B2–C2–C3 –177.8(2).

addition to a BHB bridge between the same boron centers have not been structurally characterized up to now. The folding angle between the best plane of the five-membered ring in **7b** (B1,B2,C1,C2,C3) and the B1,Si2,B2 plane [103.1(1)°] is similar to that with the B1,H,B2 plane [105(1)°].

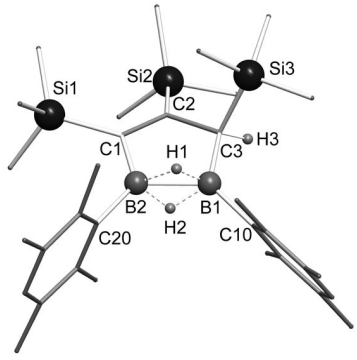

Figure 4. Structure of **7a** in the crystal, most of the hydrogen atoms have been omitted for clarity. Selected bond lengths [pm] and angles [°]: B1–B2 182.6(3), B2–C1 158.7(3), C1–C2 138.5(3), C2–C3 152.5(3), C3–B1 158.6(3), mean B–H 128(2), B–H–B 91(1), B1–C10 160.0(3), B2–C20 158.6(3), C1–Si1 187.9(2), C2–Si2 190.1(2), C3–Si3 191.2(2); B1–B2–C1 102.0(2), B1–B2–C20 129.3(2), B2–B1–C3 100.4(2), B2–B1–C10 132.3(2), B1–C3–C2 109.2(2), C3–C2–C1 114.2(2), C2–C1–B2 111.9(2), C1–B2–B1–C3 4.6(2), B2–C1–C2–C3 –14.0(2), Si1–C1–C2–C3 167.7(2), Si1–C1–C2–Si2 –26.3(3), Si2–C2–C3–Si3 89.8(2), C10–B1–B2–C20 5.5(4).

The additional carbon centers of the six-membered rings of anions **8a** (Figure 6) and **8b** originate from the former anionic center of the *n*-butyl anion of *n*-butyllithium, which was allowed to react with **1a**. They therefore carry an *n*-propyl substituent and a hydrogen atom each. Obviously, this nucleophile attacked the B–B moiety with subsequent rearrangement, including opening of the B–B bond, formation of an additional B–C bond, and migration of a hydrogen atom from carbon to boron. This hydrogen atom forms a bridge to the second boron center in **8a**, thereby leading to a short B1–B2 distance (199 pm) and strong deformation of this part of the six-membered ring: the B1,C4,B2 angle is only 76°. The plane B1,C4,B2 is inclined by 110.8(1)° to the best plane through C1,B2,B1,C3. In the contact ion pair **8b**·Li(Et_2O) (Figure 7), however, this hydrogen atom is bound to only one boron center; the B···B distance is long (244 pm) and the angle B1,C4,B2 amounts to 98°. The six-membered central ring in **8b**·Li(Et_2O) shows a twisted boat conformation.

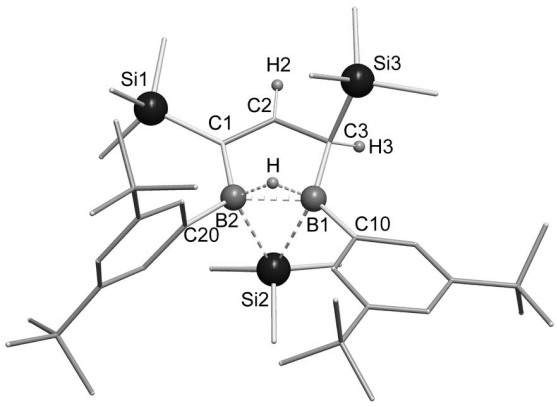

Figure 5. Structure of **7b** in the crystal, most of the hydrogen atoms have been omitted for clarity. For the two disordered *t*-butyl groups only one position is drawn. Selected bond lengths [pm] and angles [°]: B1–B2 183.2(5), B2–C1 157.7(5), C1–C2 135.2(5), C2–C3 149.3(5), C3–B1 159.4(5), B1–H 127(3), B2–H 131(3), B1–H–B2 91(2), B1–C10 156.5(5), B2–C20 160.9(5), B1–Si2 232.2(3), B2–Si2 227.1(3), B1–Si2–B2 47.0(1), C1–Si1 187.0(3), C3–Si3 191.3(3); B1–B2–C1 102.1(2), B1–B2–C20 129.6(3), B2–B1–C3 100.2(2), B2–B1–C10 130.9(3), B1–C3–C2 107.8(3), C3–C2–C1 118.6(3), C2–C1–B2 110.7(3), C1–B2–B1–C3 3.3(3), B2–C1–C2–C3 –6.2(4), Si1–C1–C2–C3 167.0(2).

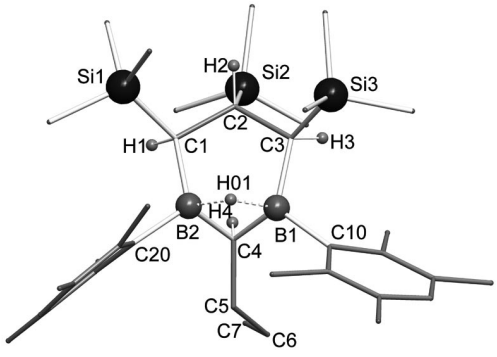

Figure 6. Structure of anion **8a** of the solvent-separated ion pair **8a**·Li(Et_2O)$_3$ in the crystal; the strongly disordered counterion [Li(Et_2O)$_3$]$^+$ and most of the hydrogen atoms have been omitted for clarity. Selected bond lengths [pm] and angles [°]: B1–B2 199.0(3), B1–H01 142(2), B2–H01 136(2), B1–H01–B2 91(1), B1–C3 164.3(3), B1–C4 159.0(3), B2–C1 163.2(3), B2–C4 162.8(3), C1–C2 157.5(2), C2–C3 158.1(2); B1–C4–B2 76.4(1), C1–B2–C4 111.1(2), C3–B1–C4 115.1(2), B2–C1–C2 110.7(1), C1–C2–C3 112.3(1), C2–C3–B1 110.4(1).

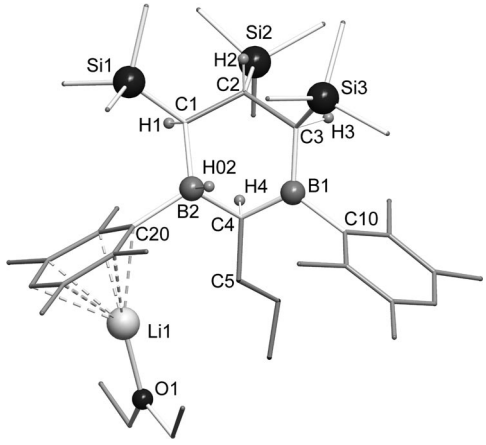

Figure 7. Structure of contact ion pair **8b**·Li(Et_2O) in the crystal; most of the hydrogen atoms have been omitted for clarity. Selected bond lengths [pm] and angles [°] (average over both independent molecules, labels of the first one): B1···B2 239.4(4), B1–C3 158.5(3), B1–C4 154.3(3), B2–C4 169.5(3), B2–C1 166.2(3), B2–H2 115(2), C1–C2 158.6(3), C2–C3 157.9(3); B1–C4–B2 95.3(2), C3–B1–C4 119.2(2), C1–B2–C4 107.4(2), B2–C1–C2 111.2(2), C1–C2–C3 116.0(2), C2–C3–B1 116.2(2), Li1–O1 190.5(4), Li–C_{Ar} 235.6(4)–244.6(4), B2–C1–C2–C3 –5.9(3), C1–C2–C3–B1 32.2(3), C2–C1–B2–C4 –50.2(2).

Computational Results

Energies and geometries of model compounds were computed at the B3LYP/6-311+G** level.[19] Nonclassical **3u** (Scheme 4) is 9.1 kcal mol^{-1} lower in energy than C_s-symmetric **1u** at this level, and nonclassical isomer **2u** is 1.8 kcal mol^{-1} higher in energy than **1u**. Values included in Scheme 1 correspond to the MP2/6-31G* level.[3] Isomer **7u** with two BHB bridges is the global minimum, and it is 18.3 kcal mol^{-1} lower in energy than **1u**.

In order to elucidate the mechanism leading to main products **5a** and **6a** of the thermolysis of **1a** and to learn the reason why derivatives of **1u** do not rearrange into derivatives of **3u** in a similar way as derivatives of **A** and **D** into those of **B** and **E**, we looked for transition states leading from **1u** to **2u** and **3u** as well as from **2u** and **3u** to **7u**, respectively.

Classical 1,2-diboracyclopentane (**1u**) transforms into **2u** in one step via transition state **TS1/2u**, which is 19.0 kcal mol^{-1} higher in energy than **1u**. Transition state **TS1/2u** closely resembles the transition state described recently for the transformation of derivatives of classical 1,2,4-triboracyclopentane into those of its nonclassical isomer **C**.[10] The transformation of **1u** into **3u**, however, like that of **A** and **D** into **B** and **E**, respectively, *cannot* take place in *one step*, since in **3u** the two bridges between the boron centers are located on opposite sides of the C,B,B,C plane. Activation of the C4–H bond via transition state **TS1/9u** leads to **9u**, which corresponds to intermediates during the transformation of **A** and **D** into **B** and **E**. This activation requires 27.7 kcal mol^{-1}, which is 8.7 kcal mol^{-1} more than the activation of the C3–H bond (through **TS1/2u**) and thus can be taken as an explanation why derivatives of **3u** are not formed in isolable amounts during the thermolysis of **1a** and **1b**. Notably, there is an alternative C4–H bond activation via transition state **TS1/10u** which is 1.7 kcal mol^{-1} lower in energy than **TS1/9u**. This route leads

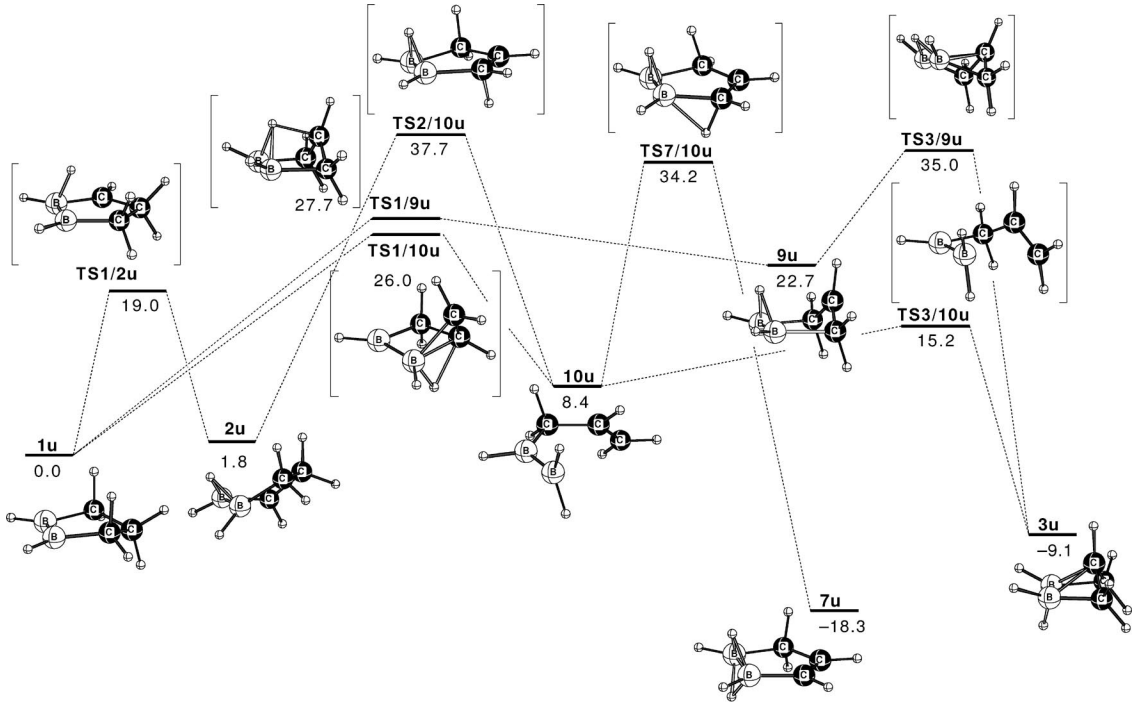

Scheme 4. Computed energies for the transformations of classical **1u** into nonclassical **2u**, **3u**, and **7u** via versatile transition states TS as computed at the B3LYP/6-311+G** level of theory. C, B, and H atoms are represented as black, white, and small white balls, respectively.

to ring-opened product **10u**, which is 8.4 kcal mol^{-1} above the energy level of **1u**. Rebuilding of the five-membered ring in **TS7/10u** requires no less than 25.8 kcal mol^{-1}, mainly because of the separation of a positive charge at a carbon center from a negative charge at the BHB unit. This charge separation is also the main reason for the high energy of **TS2/10u**. Because **TS3/10u** is computed to be 19 kcal mol^{-1} in energy lower than **TS7/10u**, derivatives of **3u** should be obtained in considerably higher amounts than those of **7u**. A direct rearrangement from **3u** into **7u** is very unlikely. Firstly, it requires a conformational change towards a classical five membered ring that generates an only singly bridged BB edge (i.e., breaking the BCB three-center bond) and also orients adjacent CH bonds favorably. Secondly, the electronic distribution should correspond to an electron-deficient BHB moiety and, consequently, to a carboanionic center. That is, the polarity must be reverse to that of **3u***, which itself is a species very high in energy. A reaction path lower in energy is the two-step process involving ring-opened intermediate **10u** (**3u** → **10u** → **7u**), which nevertheless has an energy barrier of 43.3 kcal mol^{-1}. The high yield of formation of **7b** from **1b** at ambient temperature relative to the low yield of **7a** during thermolysis of **1a** demonstrates that steric effects play a decisive role during the formation of **7a** and **7b**. Because our computations did not lead to any hint that molecules of type **3**, *our original targets*, are involved in the generation of products of type **7**, further computations on bigger models including steric effects did not make sense.

To get some insight into the mechanism of the formation of **6a**, which requires elimination of trimethylsilane in addition to cleavage of the B–B and C–C bonds, we also performed computations on models with silyl substituents at the carbon centers as well as with phenyl substituents at the boron centers. Some results are shown in Scheme 5.

Hydrogen shift in **1e** to give *trans*-**2e** is computed to be endothermic by 9.0 kcal mol^{-1} and to require 25.5 kcal mol^{-1} of activation. Nonclassical five-membered ring *trans*-**2e** opens exothermically into classical four-membered ring *trans*-**11e**. The transformation of the latter into

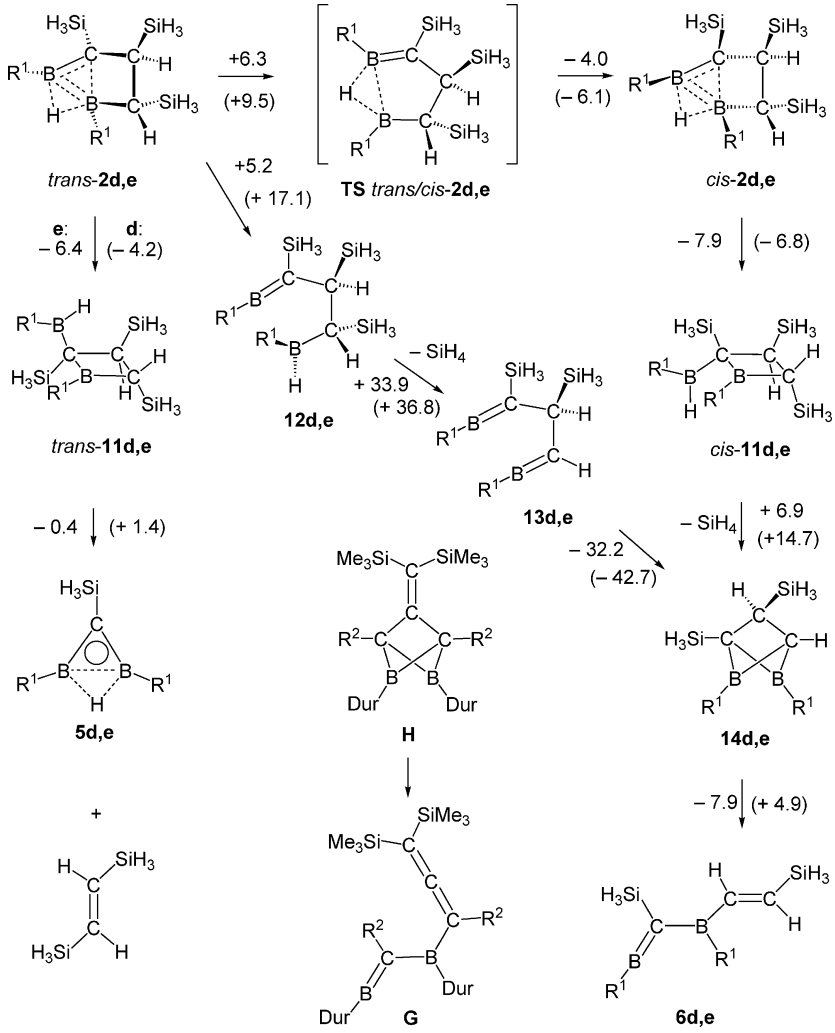

Scheme 5. Computed energies for the transformations of *trans*-**2d**,**e** (**d**: R^1 = H, **e**: R^1 = C_6H_5) into **5d**,**e** and **6d**,**e**. Values are given in kcal mol^{-1} for R^1 = C_6H_5 and in parentheses for R^1 = H. Experimentally known **H** and **G** [R^2 = CH_3, CH_2CH_3, and $CH_2C(CH_3)_3$] are shown for comparison.

5e and 1,2-disilylethene is close to thermoneutral. The structure of compound **6a** is similar to those of type **G**, which have been shown to be formed by diborabicyclobutanes of type **H**.[12,20] We therefore looked for the energetics of the 1,2-elimination of SiH_4 from ring-opened isomer **12e** of *trans*-**2e**. The former is 5.2 kcal mol^{-1} higher in energy. This elimination leading to **13e** turned out to require no less than 33.9 kcal mol^{-1}. However, low-energy routes were found starting with four-membered rings *cis*-**11d**,**e**, which were easily formed from *trans*-**2d**,**e** via transition state TS *trans*/*cis*-**2d**,**e** and *cis*-**2d**,**e**. Rearrangement from *cis*-**2e** to *cis*-**11e** occurs with a negligible barrier. Transannular 1,4-eliminations of SiH_4 from *cis*-**11e** yielding **14e** requires only 6.9 kcal mol^{-1}. The opening of **14e** into **6e** is exergonic by 7.9 kcal mol^{-1}. Thus, four-membered rings of type *trans*-**11** and *cis*-**11** are reasonable intermediates during the formation of **5a** and **6a**, which are the main products of the thermolysis of **1a**.

Conclusions

On the basis of the results obtained by computations described above, we conclude that derivatives of thermodynamically preferred isomer **3u** of **1u** cannot be prepared by thermolysis, as formation of derivatives of **2u** is preferred kinetically. The main products of the thermolysis of **1a**, compounds **5a** and **6a**, can easily be explained in analogy to known reactions. Nonclassical diborirane **5a** turned out to be a valuable starting material for the synthesis of a so-far-unknown two-electron aromatic triboracyclobutanide,[21] the first diboracyclopropane containing a planar tetracoordinate carbon center[22] and compounds with structures at the borderline between two- and three-dimensional aromaticity.[23] Finding a synthetic route to derivatives of **3u**, the neutral bishomoaromatic with the largest aromatic stabilization energy ever discussed, remains a challenge.

Experimental Section

General: Reactions were carried out under an atmosphere of dry argon by using standard Schlenk techniques. Solvents were dried, distilled, and saturated with argon. Glassware was dried with a heat gun under high vacuum. ^{1}H and ^{13}C NMR spectra were recorded with Bruker ARX 300 and Bruker AC 500 spectrometers. ^{11}B NMR spectra were recorded with a Bruker ARX 300 spectrometer. NMR references are $(CH_3)_4Si$ and $BF_3{\cdot}Et_2O$. Melting points (uncorrected) were measured under an atmosphere of argon.

1,2-Bis(2′,3′,5′,6′-tetramethylphenyl)-*all-trans*-3,4,5-tris(trimethylsilyl)-1,2-diboracyclopentane (1a): A solution of **1c** (10.6 g, 30.2 mmol) in *n*-pentane (25 mL) was added within 2 min to a slurry of (2,3,5,6-tetramethylphenyl)lithium (8.47 g, 60.4 mmol) in diethyl ether (120 mL) at –78 °C. The reaction mixture was slowly warmed to ambient temperature and all volatile components were removed in vacuo. The residue was extracted with *n*-pentane (100 mL) and the salts filtered off. Cooling to –30 °C yielded **1a** (14.8 g, 90%) in two fractions as yellow crystals. M.p. 145 °C (decomp.). ^{1}H NMR (300 MHz, C_6D_6, 300 K): δ = 0.18, 0.32 (each s, altogether 27 H, $SiMe_3$), 2.02, 2.06 (each s, 12 H, Me-Ar), 2.51 (t, $^3J_{H,H}$ = 3 Hz, 1 H, C_2CHSi), 2.73 (d, $^3J_{H,H}$ = 3 Hz, 2 H, BCHSi), 6.77 (s, 2 H, H-Ar) ppm. ^{13}C NMR (75 MHz, C_6D_6, 300 K): δ = 0.8, 1.4 (each q, Me_3Si), 19.3, 22.0 (each q, Me-Ar), 33.9 (d, $^1J_{C,H}$ = 117 Hz, C_2CHSi), 59.4 (br. d, $^1J_{C,H}$ = 101 Hz, BCHSi), 130.2 (s), 130.8 (d), 133.2 (s), 148.1 (br. s) ppm. ^{11}B NMR (96 MHz, C_6D_6, 300 K): δ = 96 ppm.

1,2-Bis(2′,3′,5′,6′-tetramethylphenyl)-3-trimethylsilyl-1,2-μ(1,2)-hydro-3-dehydro-1,2-diborirane (5a), 1,3-Bis(2′,3′,5′,6′-tetramethylphenyl)-1,3-dibora-2,5-bis(trimethylsilyl)penta-1,(*E*)-4-diene (6a), and 1,2-Bis(2′,3′,5′,6′-tetramethylphenyl)-1,2-bis(μ-hydro)-3,4,5-tris(trimethylsilyl)-1,2-diboracyclopent-3-ene (7a)

Method A: A solution of **1a** (2.0 g) in benzene (50 mL) was heated to reflux for 6 h. ^{1}H NMR spectroscopic analysis showed that the mixture contained at this time 5% unreacted **1a**, 60% **5a**, 25% **6a**, and ca. 5% **7a**.

Method B: Compound **1a** (2.3 g, 4.21 mmol) was heated in vacuo to 145 °C within 30 min and kept at this temperature for 2 min. The mixture was dissolved in hot *n*-pentane after cooling to ambient temperature. Crystallization at 0 °C and –30 °C yielded **5a** (870 mg, 55%) as colorless plates. M.p. 169 °C. Further concentration of the liquid gave a small amount of **7a** (about 5%) as a colorless solid followed by one impure crop of crystals. Compound **6a** (12%) finally crystallized at 0 °C after several days.

5a: ^{1}H NMR (300 MHz, C_6D_6, 300 K): δ = 0.35 (s, 9 H, $SiMe_3$), 2.18, 2.33 (each s, 12 H, Me-Ar), 6.97 (s, 2 H, H-Ar), 8.47 (br. s, 1 H, BHB) ppm. ^{13}C NMR (75 MHz, $CDCl_3$, 300 K): δ = 0.5 ($SiMe_3$), 19.8, 20.0 (Me-Ar), 131.1 (br., CB), 132.2, 133.3 (C_{Ar}), 133.6 (CB), 136.5 (C_{Ar}) ppm. ^{11}B NMR (96 MHz, $CDCl_3$, 300 K): δ = 29 ppm.

6a: ^{1}H NMR (300 MHz, CD_2Cl_2, 295 K): δ = –0.9, 0.0 (each s, 9 H, $SiMe_3$), 2.17, 2.30 (each s, 12 H, Me-Ar), 6.46 (d, $^3J_{H,H}$ = 21 Hz, 1 H, HC=C), 6.96 (s, 2 H, H-Ar), 7.09 (d, $^3J_{H,H}$ = 21 Hz, 1 H, HC=C) ppm. ^{13}C NMR (75 MHz, CD_2Cl_2, 300 K): δ = –1.7, 2.7 ($SiMe_3$), 19.6, 20.4 (Me-Ar), 86.6 (br., –80 °C, C=B), 133.6, 133.9, 138.1, 138.6 (C_{Ar}), 151.9 (d, $^1J_{C,H}$ = 134 Hz, BC=*C*), 156.1 (br. d, $^1J_{C,H}$ = 133 Hz, B*C*=C) ppm. ^{11}B NMR (96 MHz, CD_2Cl_2, 300 K): δ = 69 ppm.

7a: ^{1}H NMR (300 MHz, $CDCl_3$, 300 K): δ = 0.02, 0.04, 0.39 (each s, 9 H, $SiMe_3$), 2.00, 2.12, 2.15, 2.19, 2.20, 2.22, 2.36 (each s, altogether 24 H, Me-Ar), 2.53 (br. s, 1 H, BHB), 3.53 (s, 1 H, BCHSi), 3.63 (br. s, 1 H, BH′B), 6.86, 6.87 (each s, 1 H, H-Ar) ppm. ^{13}C NMR (75 MHz, $CDCl_3$, 300 K): δ = –0.1, 2.5, 3.4 ($SiMe_3$), 19.6, 19.7, 20.0, 20.2, 20.2, 20.5, 21.2, 22.0 (Me-Ar), 55.7 (br., BCHSi), 131.1, 131.3, 132.8, 132.8, 133.0, 133.0, 135.0, 135.5, 136.0, 137.1 (C_{Ar}), 159.7 [br., B*C*(Si)=C], 193.1 [BC(Si)=*C*] ppm. ^{11}B NMR (96 MHz, $CDCl_3$, 300 K): δ = 23 ppm.

1,2-Bis(3′,5′-di-*tert*-butylphenyl)-1,2-μ-hydro-1,2-μ-trimethylsilyl-3,5-bis(trimethylsilyl)-1,2-diboracyclopent-3-ene (7b): Diethyl ether (10 mL) was added to a solution of **1c** (2.98 g, 8.49 mmol) in *n*-pentane (50 mL) at –78 °C, followed by a solution of (3,5-di-*tert*-butylphenyl)lithium (0.75 N in diethyl ether, 22.6 mL). After warming to room temperature, all volatile components were removed in vacuo, and the residue was suspended in *n*-pentane (50 mL) and stirred for 3 d. Insoluble byproducts were filtered off, and the solution was concentrated to 20 mL. Crystallization at –30 °C gave **7b** (3.52 g, 63%) as colorless crystals. M.p. 130 °C (decomp.). ^{1}H NMR (300 MHz, C_6D_6, 300 K): δ = 0.05, 0.20, 0.26 (each s, 9 H, $SiMe_3$), 1.32 (s, 18 H, *t*Bu), 1.49 (s, 18 H, *t*Bu), 2.9 (br. s, 1 H, BHB), 2.93 (m, 1 H, BCHSi), 7.52 (t, 1 H, H-Ar), 7.57 (d, 2 H, H-Ar), 7.59 (t, 1 H, H-Ar), 7.71 (m, 1 H, C_2CH), 7.81 (d, 2 H, H-Ar) ppm. ^{13}C NMR (75 MHz, C_6D_6, 300 K): δ = –1.0, 0.9, 3.8 (Me_3Si),

31.6, 31.9, 34.9, 35.1 (*t*Bu), 45.7 (br. d, $^1J_{C,H}$ = 124 Hz, BCHSi), 121.1, 122.4, 128.7, 129.8, 149.4, 149.7, 164.1 (d, $^1J_{C,H}$ = 156 Hz, C_2CH) ppm; signals for the *ipso*-C-Ar and B*C*CSi atoms were not observed. ^{11}B NMR (96 MHz, C_6D_6, 300 K): δ = 27 ppm.

Lithium 1,3-Bis(2′,3′,5′,6′-tetramethylphenyl)-1,3-μ-hydrido-2-propyl-*cis*-4-*trans*-5-*cis*-6-tris(trimethylsilyl)-1,3-diboracyclohexane [8a·Li(Et$_2$O)$_3$] and Lithium 1,3-Bis(2′,3′,5′,6′-tetramethylphenyl)-1-hydrido-2-propyl-*cis*-4-*trans*-5-*cis*-6-tris(trimethylsilyl)-1-borata-3-boracyclohexane [8b·Li(Et$_2$O)]: A solution of **1a** (900 mg, 1.65 mmol) in diethyl ether (30 mL) was treated with a solution of *n*-butyllithium (1.6 M in hexanes, 2.1 mL) at 0 °C. After warming to room temperature, all volatile components were removed in vacuo, and the residue was dissolved in *n*-pentane and crystallized at 0 °C to give of **8b**·Li(Et$_2$O) (800 mg, 71%) as colorless needles. Cooling a diethyl ether solution of **8b**·Li(Et$_2$O) to –30 °C gave **8a**·Li(Et$_2$O)$_3$ as colorless crystals.

8a·Li(Et$_2$O)$_3$: ^{1}H NMR (500 MHz, [D$_{10}$]Et$_2$O, 293 K): δ = –0.36, 0.09 (each s, altogether 27 H, SiMe$_3$), 0.44 (m, 2 H, CH$_2$), 0.60 (m, 1 H, B$_2$CH), 0.68 (t, 3 H, CH$_2$*C*H$_3$), 0.73, (m, 2 H, BCHSi), 1.07 (m, 2 H, CH$_2$), 1.27 (1 H, C$_2$CHSi), 1.41 (m, BHB), 2.13, 2.14, 2.51 (each s, altogether 24 H, Me-Ar), 6.64 (s, 2 H, H-Ar) ppm. ^{13}C NMR (125 MHz, [D$_{10}$]Et$_2$O, 293 K): δ = 1.4, 1.5 (SiMe$_3$), 15.5 (CH$_2$*C*H$_3$, overlaid by [D$_{10}$]Et$_2$O), 20.9, 21.2, 21.3, 24.0 (Me-Ar), 21.0 (BCHSi), 21.6 (C$_2$*C*HSi), 25.5 (CH$_2$), 27.8 (B$_2$CH), 38.5 (CH$_2$), 128.3, 132.2, 133.3, 137.3, 140.5 (C$_{Ar}$), 155.5 (br., BC$_{Ar}$) ppm. ^{11}B NMR (160 MHz, [D$_{10}$]Et$_2$O, 293 K): δ = 3 ppm.

8b·Li(Et$_2$O): M.p. 58 °C (decomp.). ^{1}H NMR (300 MHz, C_6D_6, 293 K): δ = 0.22 (s, 18 H, SiMe$_3$), 0.36 (m, 2 H, *C*H$_2$CH$_3$), 0.49 (t, 6 H, Et$_2$O), 0.58 (s, 9 H, SiMe$_3$), 0.71 (t, 3 H, CH$_2$*C*H$_3$), 1.25 (m, 4 H, B$_2$CH*C*H$_2$ and BCHSi), 1.53 (m, 1 H, B$_2$*C*HCH$_2$), 1.89 (m, 1 H, C$_2$CHSi), 2.10, 2.13 (each s, 6 H, Me-Ar), 2.45 (m, 1 H, HB), 2.56 (t, 4 H, Et$_2$O), 2.65, 2.76 (each s, 6 H, Me-Ar), 6.67 (s, 2 H, H-Ar) ppm. ^{13}C NMR (75 MHz, C_6D_6, 293 K): δ = 1.0, 1.9 (Me$_3$Si), 14.1 (Et$_2$O), 15.1 (CH$_2$*C*H$_3$), 20.5, 20.5, 21.0 (Me-Ar), 21.2 (B$_2$*C*HCH$_2$), 21.3 (br. d, BCHSi), 23.0 (Me-Ar), 24.9 (*C*H$_2$CH$_3$), 33.4 (C$_2$*C*HSi), 38.7 (B$_2$CH*C*H$_2$), 65.9 (Et$_2$O), 128.3, 133.0, 133.2, 136.9, 138.6 (C$_{Ar}$), 157.8 (br., BC$_{Ar}$) ppm. ^{11}B NMR (96 MHz, C_6D_6, 293 K): δ = 21 ppm.

X-ray Crystal Structure Analyses: Single crystals were grown from *n*-pentane solutions at 0 °C [**6a**, **8b**·Li(Et$_2$O)] and –30 °C (**1a**, **5a**, **7a**,**b**). Single crystals of **8a**·Li(Et$_2$O)$_3$ were grown from diethyl ether at –30 °C. These crystals were investigated on imaging plate systems (IPDS Stoe) by using graphite monochromated Mo-K_α radiation at 193 K. The space groups were determined from the systematic absences and intensity statistics; no absorption corrections were applied. The structures were solved by direct methods and refined against all F^2 data by using full-matrix least-squares and difference Fourier techniques (SHELX programs[24,25]). Most hydrogen atoms were kept riding on calculated positions with isotropic displacement factors taken as 1.2 times (1.5 times for CH$_3$) the U_{eq} value of the corresponding C atom. The hydrogen atoms at the central rings were located and refined with individual isotropic displacement factors. For all heavier atoms anisotropic displacement parameters were used. The structure of **7a**·0.5Et$_2$O shows disorder of the solvent ether molecule on a center of symmetry. In **8a**·Li(Et$_2$O)$_3$, two of the ether molecules are disordered over two alternative positions, in the third one a methyl group is disordered. The *n*-propyl rest of the anion shows also disorder of the final methyl group. The structure of **8b**·Li(Et$_2$O) has two crystallographically independent molecules of very similar conformation. Thus, average values were used for the geometrical data. Details of the experimen-

Table 1. Crystal and experimental data for the structure determinations of **1a**, **5a**, **6a**, and **7a**·0.5Et$_2$O.

	1a	**5a**	**6a**	**7a**·0.5Et$_2$O
Empirical formula	$C_{32}H_{56}B_2Si_3$	$C_{24}H_{36}B_2Si$	$C_{29}H_{46}B_2Si_2$	$C_{34}H_{61}B_2O_{0.5}Si_3$
Formula weight	546.66	374.24	472.46	583.72
Measuring temperature	193 K	193 K	193 K	193 K
Crystal system	monoclinic	monoclinic	triclinic	monoclinic
Space group	$P2_1/n$	$P2_1/n$	$P\bar{1}$	$P2_1/c$
a [pm]	964.4(1)	934.2(1)	997.9(1)	1665.0(1)
b [pm]	2078.8(1)	1967.9(1)	1172.3(1)	936.77(4)
c [pm]	1733.9(1)	1332.2(1)	1502.7(2)	2374.1(2)
α [°]			78.77(1)	
β [°]	93.26(1)	95.68(1)	72.66(1)	91.799(8)
γ [°]			66.81(1)	
Volume [Å^3]	3470.5(4)	2437.1(3)	1531.9(3)	3701.1(4)
Z	4	4	2	4
Calculated density [g cm^{-3}]	1.046	1.020	1.024	1.048
Absorption coefficient [mm^{-1}]	0.155	0.102	0.130	0.150
F(000)	1200	816	516	1284
Crystal size [mm]	0.40 × 0.30 × 0.10	0.60 × 0.30 × 0.25	0.65 × 0.35 × 0.10	0.78 × 0.15 × 0.08
Θ_{max} [°]	25.91	24.91	24.82	25.91
Index range	–11/11	–11/11	–11/11	–20/20
	–23/24	–23/23	–13/13	–11/10
	–21/21	–15/15	–17/17	–29/29
Scan type	ϕ-scans	ϕ-scans	ω-scans	ϕ-scans
No. of reflections	27046	18152	18132	28304
Unique refl. (R_{int})	6521 (0.053)	4221 (0.056)	5246 (0.077)	6991 (0.092)
Observed refl. [$I > 2\sigma(I)$]	4614	3316	4185	4128
Parameters, data/param. ratio	363, 18.0	259, 16.3	320, 16.4	396, 17.7
Goodness-of-fit (F^2)	0.915	1.058	1.064	0.862
R [$I > 2\sigma(I)$]	0.0393	0.0410	0.0459	0.0532
wR_2 (all refl.)	0.0978	0.1200	0.1396	0.0952
Largest diff. peak/hole [e Å^{-3}]	+0.263/–0.199	+0.211/–0.221	+0.528/–0.464	+0.282/–0.167

Table 2. Crystal and experimental data for the structure determinations of **7b**, **8a**·Li(Et_2O)$_3$, and **8b**·Li(Et_2O).

	7b	**8a**·Li(Et_2O)$_3$	**8b**·Li(Et_2O)
Empirical formula	$C_{40}H_{72}B_2Si_3$	$C_{48}H_{95}B_2LiO_3Si_3$	$C_{40}H_{75}B_2LiOSi_3$
Formula weight	658.87	833.07	684.83
Measuring temperature	193 K	193 K	193 K
Crystal system	orthorhombic	triclinic	triclinic
Space group	$P2_12_12_1$	$P\bar{1}$	$P\bar{1}$
a [pm]	940.83(5)	1178.2(1)	1303.38(8)
b [pm]	1184.16(6)	1335.6(1)	1880.5(1)
c [pm]	3930.5(1)	1849.1(2)	2012.7(1)
α [°]		76.85(1)	65.914(6)
β [°]		76.28(1)	86.841(7)
γ [°]		85.18(1)	89.764(7)
Volume [Å^3]	4378.9(6)	2751.2(4)	4496(1)
Z	4	2	4
Calculated density [g cm^{-3}]	0.999	1.006	1.012
Absorption coefficient [mm]$^{-1}$	0.132	0.120	0.132
F(000)	1456	924	1512
Crystal size [mm]	0.65 × 0.20 × 0.05	0.60 × 0.45 × 0.30	0.40 × 0.35 × 0.20
Θ_{max} [°]	25.95	26.31	25.94
Index range	–11/11	–14/13	–15/16
	–14/12	–16/15	–23/23
	–45/45	–22/22	–24/24
Scan type	ϕ-scans	ω-scans	ϕ-scans
No. of reflections	21467	29554	44613
Unique refl., (R_{int})	7519 (0.075)	11053 (0.030)	16312 (0.045)
Observed refl. [$I > 2\sigma(I)$]	5435	6666	9521
Parameters, data/param. ratio	501, 15.0	637, 17.4	922, 17.7
Goodness-of-fit (F^2)	0.936	0.954	0.947
R [$I > 2\sigma(I)$]	0.0532	0.0448	0.0461
wR_2 (all refl.)	0.1293	0.1153	0.1088
Largest diff. peak/hole [e Å^{-3}]	+0.532/–0.333	+0.340/–0.345	+0.708/–0.392

tal and crystal data are summarized in Tables 1 and 2. CCDC-292769 (for **1a**), -292770 (for **5a**), -292773 (for **6a**), -292774 (for **7a**·0.5Et_2O), -292771 (for **7b**), -292768 [for **8a**·Li(Et_2O)$_3$], and 292772 [for **8b**·Li(Et_2O)] contain the supplementary crystallographic data for this paper. These data can be obtained free of charge from The Cambridge Crystallographic Data Centre via www.ccdc.cam.ac.uk/data_request/cif.

Acknowledgments

This work was supported by the Deutsche Forschungsgemeinschaft (FSP Polyeder) and the Fonds der Chemischen Industrie.

[1] G. E. Herberich, C. Ganter, L. Wesemann, *Chem. Ber.* **1990**, *123*, 49–51; G. Knörzer, H. Seyffer, W. Siebert, *Z. Naturforsch., Teil B* **1990**, *45*, 1136–1138; G. E. Herberich, C. Ganter, L. Wesemann, R. Boese, *Angew. Chem.* **1990**, *102*, 914–915; *Angew. Chem. Int. Ed. Engl.* **1990**, *29*, 912–913.

[2] C. Präsang, Y. Sahin, M. Hofmann, G. Geiseler, W. Massa, A. Berndt, *Eur. J. Inorg. Chem.* **2004**, 3063–3073.

[3] D. Steiner, C. Balzereit, H.-J. Winkler, N. Stamatis, M. Hofmann, P. von Ragué Schleyer, W. Massa, A. Berndt, *Angew. Chem.* **1994**, *106*, 2391–2394; *Angew. Chem. Int. Ed. Engl.* **1994**, *33*, 2303–2306.

[4] C. Präsang, P. Amseis, D. Scheschkewitz, G. Geiseler, W. Massa, M. Hofmann, A. Berndt, *Angew. Chem.* **2006**, *118*, 6897–6899; *Angew. Chem. Int. Ed.* **2006**, *45*, 6745–6747.

[5] M. Hofmann, D. Scheschkewitz, A. Ghaffari, G. Geiseler, W. Massa, H. F. Schaefer III, A. Berndt, *J. Mol. Model.* **2000**, *6*, 257–271.

[6] D. Scheschkewitz, A. Ghaffari, P. Amseis, M. Unverzagt, G. Subramanian, M. Hofmann, P. von Ragué Schleyer, H. F. Schaefer III, G. Geiseler, W. Massa, A. Berndt, *Angew. Chem.* **2000**, *112*, 1329–1332; *Angew. Chem. Int. Ed.* **2000**, *39*, 1272–1275.

[7] The bishomoaromatic stabilization energy of **4u** is smaller than that of the isoelectronic anion containing a pentacoordinate silicon instead of the pentacoordinate carbon center (71.4 kcal mol^{-1} at this level).[8] This is to be expected because of the more unsymmetrical delocalization in **4a** due to the bigger difference in electronegativity between boron and carbon than between boron and silicon centers.[8]

[8] D. Scheschkewitz, M. Hofmann, A. Ghaffari, P. Amseis, C. Präsang, W. Mesbah, G. Geiseler, W. Massa, A. Berndt, *J. Organomet. Chem.* **2002**, *646*, 262–270.

[9] Y. Sahin, A. Ziegler, T. Happel, H. Meyer, M. J. Bayer, H. Pritzkow, W. Massa, M. Hofmann, P. von Ragué Schleyer, W. Siebert, A. Berndt, *J. Organomet. Chem.* **2003**, *680*, 244–256.

[10] D. Scheschkewitz, P. Amseis, G. Geiseler, W. Massa, M. Hofmann, A. Berndt, *Eur. J. Inorg. Chem.* **2005**, 4078–4085.

[11] M. Menzel, D. Steiner, H.-J. Winkler, D. Schweikart, S. Mehle, S. Fau, G. Frenking, W. Massa, A. Berndt, *Angew. Chem.* **1995**, *107*, 368–370; *Angew. Chem. Int. Ed. Engl.* **1995**, *34*, 327–329.

[12] M. Menzel, H.-J. Winkler, T. Ablelom, D. Steiner, S. Fau, G. Frenking, W. Massa, A. Berndt, *Angew. Chem.* **1995**, *107*, 1476–1479; *Angew. Chem. Int. Ed. Engl.* **1995**, *34*, 1340–1343.

[13] H. H. Lindner, T. Onak, *J. Am. Chem. Soc.* **1966**, *88*, 1890–1894.

[14] A. Berndt, *Angew. Chem.* **1993**, *105*, 1034–1058; *Angew. Chem. Int. Ed. Engl.* **1993**, *32*, 985–1009.

[15] The C=C–Si bond angle of only 109°[14] observed for a borylmethyleneborane similar to **6a**, which is, however, sterically more hindered because of a mesityl substituent at the position of the α-vinyl hydrogen in **6a**, is therefore in part the consequence of distortion due to steric hindrance.

[16] T. Müller, M. Juhasz, C. A. Reed, *Angew. Chem.* **2004**, *116*, 1569–1572; *Angew. Chem. Int. Ed.* **2004**, *43*, 1543–1546.

[17] P. Paetzold, U. Englert, R. Finger, T. Schmitz, A. Tapper, R. Ziembinski, *Z. Anorg. Allg. Chem.* **2004**, *630*, 508–518 and the literature cited therein.

[18] J. C. Calabrese, L. F. Dahl, *J. Am. Chem. Soc.* **1971**, *93*, 6042–6047.

[19] All structures were optimized at the B3LYP/6-311+G** level of density functional theory: A. D. Becke, *J. Chem. Phys.* **1993**, *98*, 5648–5652, C. Lee, W. Yang, R. G. Parr, *Phys. Rev. B* **1988**, *37*, 785–789. The nature of the stationary points was characterized by frequency calculations and relative energies were corrected for zero-point vibrational energies. Gaussian03 was used throughout: M. J. Frisch, G. W. Trucks, H. B. Schlegel, G. E. Scuseria, M. A. Robb, J. R. Cheeseman, J. A. Montgomery Jr, T. Vreven, K. N. Kudin, J. C. Burant, J. M. Millam, S. S. Iyengar, J. Tomasi, V. Barone, B. Mennucci, M. Cossi, G. Scalmani, N. Rega, G. A. Petersson, H. Nakatsuji, M. Hada, M. Ehara, K. Toyota, R. Fukuda, J. Hasegawa, M. Ishida, T. Nakajima, Y. Honda, O. Kitao, H. Nakai, M. Klene, X. Li, J. E. Knox, H. P. Hratchian, J. B. Cross, V. Bakken, C. Adamo, J. Jaramillo, R. Gomperts, R. E. Stratmann, O. Yazyev, A. J. Austin, R. Cammi, C. Pomelli, J. W. Ochterski, P. Y. Ayala, K. Morokuma, G. A. Voth, P. Salvador, J. J. Dannenberg, V. G. Zakrzewski, S. Dapprich, A. D. Daniels, M. C. Strain, O. Farkas, D. K. Malick, A. D. Rabuck, K. Raghavachari, J. B. Foresman, J. V. Ortiz, Q. Cui, A. G. Baboul, S. Clifford, J. Cioslowski, B. B. Stefanov, G. Liu, A. Liashenko, P. Piskorz, I. Komaromi, R. L. Martin, D. J. Fox, T. Keith, M. A. Al-Laham, C. Y. Peng, A. Nanayakkara, M. Challacombe, P. M. W. Gill, B. Johnson, W. Chen, M. W. Wong, C. Gonzalez, J. A. Pople, Gaussian 03, Revision B.03, Gaussian, Inc., Wallingford CT, **2004**.

[20] M. Menzel, C. Wieczorek, S. Mehle, J. Allwohn, H.-J. Winkler, M. Unverzagt, M. Hofmann, P. von Rague Schleyer, S. Berger, W. Massa, A. Berndt, *Angew. Chem.* **1995**, *107*, 728–731; *Angew. Chem. Int. Ed. Engl.* **1995**, *34*, 657–660.

[21] Y. Sahin, C. Präsang, P. Amseis, M. Hofmann, G. Geiseler, W. Massa, A. Berndt, *Angew. Chem.* **2003**, *115*, 693–695; *Angew. Chem. Int. Ed.* **2003**, *42*, 669–671.

[22] Y. Sahin, C. Präsang, M. Hofmann, G. Subramanian, G. Geiseler, W. Massa, A. Berndt, *Angew. Chem.* **2003**, *115*, 695–698; *Angew. Chem. Int. Ed.* **2003**, *42*, 671–674.

[23] Y. Sahin, C. Präsang, M. Hofmann, G. Geiseler, W. Massa, A. Berndt, *Angew. Chem.* **2005**, *117*, 1670–1673; *Angew. Chem. Int. Ed.* **2005**, *44*, 1643–1646.

[24] G. M. Sheldrick, *SHELXS-97: Program for the Solution of Crystal Structures*, University of Göttingen, **1997**.

[25] G. M. Sheldrick, *SHELXL-97: Program for the Refinement of Crystal Structures*, University of Göttingen, **1997**.

Received: June 19, 2008
Published Online: October 9, 2008

